

L-Band Lamb mode resonators in Gallium Nitride MMIC technology

Laura C. Popa, Dana Weinstein

Massachusetts Institute of Technology, Cambridge, MA/USA

E-mail: lpopa@mit.edu

Abstract—We present a theoretical and experimental study of L-band (1-2 GHz) Lamb mode resonators in Gallium Nitride (GaN) monolithic microwave IC technology. These resonators leverage Au-free metallization and optimized anchors, enabling fQ products up to 5.5×10^{12} , the highest reported in GaN resonators to date. These devices also demonstrate the highest electromechanical coupling (k_{eff}^2 of 0.39%) measured in GaN resonators using an interdigitated transducer in the absence of a bottom electrode. Achieving such high values of fQ and k_{eff}^2 , these GaN MEMS resonators can enable channel select filters for wireless communications, with wide bandwidth tuning capabilities (0.18 – 0.8 MHz) at 1-2 GHz range.

Keywords—gallium nitride, III-V, piezoelectricity, MEMS resonators, Lamb mode resonator.

I. MOTIVATION

Over the past few years, the transition to third and fourth generation (3G, 4G) wireless communications has led to an increase in demand for higher bandwidth wireless data transfer with unprecedented frequency selectivity. As a result, telecommunications systems such as Global System for Mobile (GSM) or Code Division Multiple Access (CDMA) have been partially replaced by networks that allow higher data transfer rates and multiple users per band. One such technology is the Long Term Evolution (LTE) system [1], characterized by broadband data transfer through multiple narrow bandwidth subcarriers. Multiple LTE frequency bands have been released in the ultra-high-frequency range. In order to achieve cost-efficient data transfer rates, these LTE radio access networks can benefit from efficient hardware, including both front-end filters and reliable frequency sources for clocking. With quality factors exceeding 5,000 at GHz frequencies, small footprints, and the ability to achieve multiple frequencies on the same chip, MEMS resonators can provide solutions for low loss narrow bandwidth filters and low phase-noise oscillators for operation over a wide frequency range.

MEMS resonators also have the capacity for monolithic integration with standard integrated circuits, which has the benefit of reduced size, weight, and power, improved parasitics, and reduced impedance matching constraints, particularly at high frequencies. A lot of effort has gone into CMOS integration of MEMS resonators [2,3]. However, for high power, high frequency applications, III-V monolithic microwave ICs (MMICs) are increasingly dominating the market. As a wide bandgap semiconductor, GaN provides high electron velocities, charge densities ($1 \times 10^{13} \text{ cm}^{-2}$ in AlGaIn/GaN), and critical electric fields, ideal for high

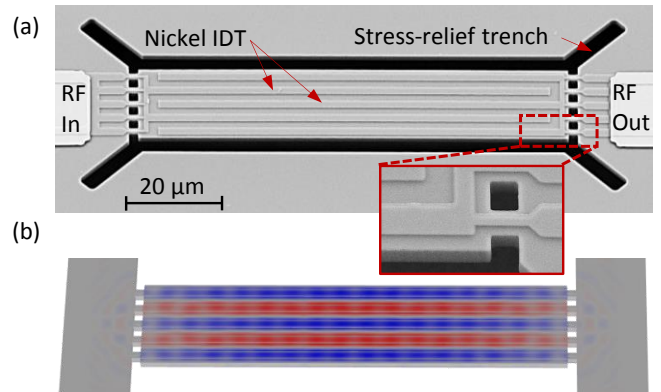


Figure 1. (a) SEM of GaN IDT resonator in MMIC technology. (b) 3D Comsol simulation of S_0 Lamb mode showing stress fields.

power ($>10 \text{ W/mm}$), high frequency ($>300 \text{ GHz}$) ICs. GaN also exhibits high piezoelectric coefficients (electromechanical coupling k_{eff}^2 up to 2% in FBARs) while at the same time having high acoustic velocities and low acoustic losses.

The authors have previously demonstrated high performance passive and active (HEMT-sensed) GaN resonators from 200 MHz to 3.5 GHz in both flexural and contour modes [4]. Successful implementation of MEMS resonators for clocking and tunable bandwidth filters requires high quality factor (Q), high electromechanical coupling (k_{eff}^2) devices, with multiple frequencies on the same chip and excellent power handling. To this end, this work focuses on the optimization of transduction efficiency, electrode metallization, and anchor design of contour mode resonators in *standard* GaN MMIC technology.

II. DESIGN CONSIDERATIONS

In a monolithically integrated solution, various constraints of the technology must be considered when optimizing the design of the MEMS resonators. There are three key considerations by which we optimize our design:

1. GaN thickness: the thickness of the GaN MMIC heterostructure is set by the foundry to maximize charge density and mobility at the interface of GaN with a top Al-GaN layer, where the channel of a High Electron Mobility Transistor (HEMT) is formed.
2. Bottom electrode: due to the epitaxial growth process and RF requirements of the substrate, MMIC technology prohibits the use of bottom electrodes, more commonly found in sputtered piezoelectric materials, (e.g. AlN). While bottom electrode configurations can be realized

through post-processing [5], these additional steps would lead to extra cost, reduced yield, and lower resonator Q .

3. Residual stress: cooling down from high growth temperatures (800-1100°C), GaN and the (111) Si substrate compress at different rates due to different thermal expansion coefficients [6], leading to residual stress in the GaN film. In the case of released structures, this can affect the mechanical properties of the resonators and even lead to cracking and breaking. Careful design of the resonator cavities and anchors can alleviate these issues.

To achieve high performance resonators with multiple frequencies on the same chip within this technology, we designed 5th order extensional resonators driven piezoelectrically with a top metal interdigitated transducer (IDT) as shown in Fig. 1(a). Contrary to [4], in this work we remove the AlGaIn barrier layer and the 2DEG, allowing transduction through the entire GaN. For efficient electromechanical coupling using a transducer with no bottom electrode, this work targets the zero-order symmetric Lamb mode (S_0) [7]. Fig. 1(b) shows the 3D simulation of a 1 GHz S_0 resonant mode. This design has the advantage of higher Q relative to bottom-electrode devices, since an additional metal electrode would lead to mass loading, distortion of the mode and increased acoustic loss through interfacial scattering [8].

To prevent the formation of fractures at points of maximum stress, 45°-oriented trenches have been etched through the GaN film, in order to discontinue the released membrane around the resonator. Stress can be further relieved by using multiple suspension beams to the resonator (Fig. 1). Using multiple anchor points also has the benefit of higher Q , suppressed spurious modes, and increased power handling [9].

III. FABRICATION

Devices were fabricated at MIT using Raytheon’s standard MMIC GaN heterostructure, comprised of Molecular Beam Epitaxy (MBE) AlGaIn(25nm)/GaN(1.7 μ m) on (111)-Si using a thin AlN nucleation layer (Fig. 2(a)). MBE was chosen over Molecular Organic Chemical Vapor Deposition (MOCVD) growth due to reduced process temperatures, leading to lower residual stresses [6]. The choice of silicon as a substrate for growth was motivated by a reduced cost, compared to silicon carbide or sapphire, as well as for reduced complexity of the final release step.

This is the first implementation of GaN MEMS resonator

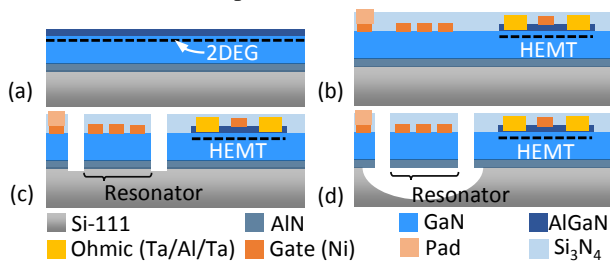


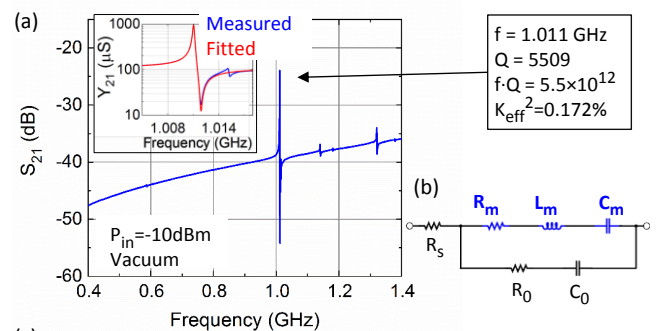
Figure 2. GaN IDT resonators are fabricated in Au-free standard HEMT process with two additional steps for defining the acoustic cavity and for the final release.

tors in an Au-free HEMT process flow. While typical HEMT MMIC processes use Au electrodes to make contact to the 2DEG channel and for low-resistance transistor gates, many efforts have been made to realize Au-free metallization schemes in order to allow for the integration of GaN MMICs in CMOS foundries [10]. Eliminating Au-electrodes from the resonators also allows for higher resonator quality factors, since Au is known to lead to additional dissipation through mass loading, phonon-electron scattering and interfacial losses.

The fabrication process involved a subset of a GaN HEMT flow with only two additional steps. Processing starts with a shallow AlGaIn etch in a BCl_3/Cl_2 chemistry which removes the 2D electron gas (2DEG) between the AlGaIn/GaN layers to allow for transduction through the volume of the entire GaN film. The gate metal of the transistor (100 nm of Nickel) is then used to define piezoelectric IDTs (Fig. 2(b)). Since these devices are processed side by side with GaN HEMTs, a PECVD Si_3N_4 layer (150 nm) is deposited to passivate the surface and protect the 2DEG channel. Metal pads (50 nm Ti/300 nm Au) are connected to the gate electrodes through vias in the passivation layer. A deep Cl_2 GaN etch in an inductively coupled plasma (Fig. 2(c)) defines the acoustic cavities. Finally, a XeF_2 silicon etch releases the resonators (Fig. 2(d)).

IV. EXPERIMENTAL RESULTS

Resonators were measured in vacuum on a Cascade RF probe station, using a standard 2-port measurement on an Agilent Parametric Network Analyzer, and de-embedded using an on-chip Open structure. The measured frequency response of the resonator in Fig. 1(a) is shown in Fig. 3(a). In Fig. 3(b), the equivalent circuit used to model the device is shown. This Modified Butterworth Model (MBVD) includes a mechanical RLC branch, capacitive and resistive feedthrough, as well as the series resistance of the drive



	R_m (k Ω)	L_m (mH)	C_m (aF)	Q_m	C_0 (fF)	R_0 (k Ω)	R_s (Ω)	Q_L	k_{eff}^2 (%)	FOM
5-beam	1.0	0.87	28.6	5509	17	0.58	29.5	5344	0.172	9.2
3-beam	2.1	0.99	24.7	2951	18	1.48	31.4	2909	0.166	4.8

Figure 3. (a) Measured frequency response of resonator in Fig. 1. (b) Modified Butterworth Van-Dyke Model is used to fit the data. (c) Fitted parameters of 5-beam resonator and 3-beam resonator, respectively are shown.

electrodes. The 5-tether device introduced in Fig. 1 shows a mechanical quality factor Q_m of 5509 at 1.011 GHz, with an $f \cdot Q_m$ of 5.5×10^{12} , the highest measured in GaN to date, enabling filters with bandwidth as low as 180 kHz. A similar device but with only 3 tethers has also been tested. The extracted parameters for both of these devices are shown in Fig 3(c). As discussed above, the mechanical quality factor of this second resonator is lower than in the case of the 5-beam design.

For each of these devices, Q_L is the electrically loaded quality factor and k_{eff}^2 is given by:

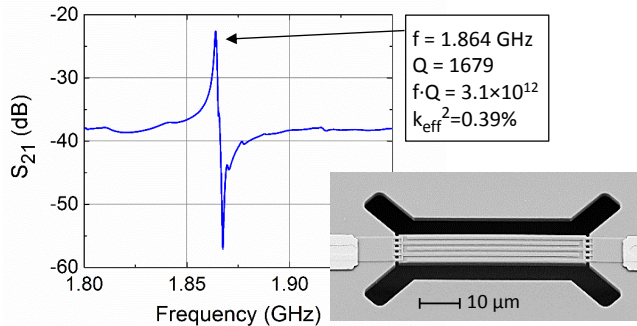
$$k_{eff}^2 = 1 - \frac{f_s^2}{f_p^2}. \quad (1)$$

Here, f_s and f_p are the resonance and anti-resonance frequencies, respectively, and the relevant figure of merit is [11]:

$$FOM = \frac{k_{eff}^2 Q_L}{1 - k_{eff}^2}. \quad (2)$$

Scaling to higher frequency, Fig. 4 shows a device with resonance at 1.864 GHz and Q_m of 1679. This device has k_{eff}^2 of 0.39%, the highest measured in GaN using IDTs with no bottom electrode, enabling up to 0.8% bandwidth filters. Extracted parameters using the same equivalent circuit model as in the case of the 1GHz resonators are given for devices with three different anchor lengths. The device designed with ‘‘Anchor 1’’ shows the highest Q_m of the three, which implies that the length of the tethers matches closest to quarter wavelength for the S_0 mode. Devices with Anchor 2 and 3 have tethers that are 100 nm shorter and longer, respectively, than Anchor 1. These three resonators have comparable value of k_{eff}^2 , with $f \cdot Q_m$ values higher than any previously reported GaN resonators to date.

To explore the fundamental limit of transduction of the S_0 mode in GaN, we simulated the dependence of k_{eff}^2 on frequency, or equivalently, on the normalized thickness (h/λ) as shown in Fig. 5. The measured k_{eff}^2 of the resonators



	R_m (k Ω)	L_m (mH)	C_m (aF)	Q_m	C_0 (fF)	R_0 (k Ω)	R_S (Ω)	Q_L	k_{eff}^2 (%)	FOM
Anch. 1	1.3	0.2	36.3	1854	10.7	0.84	31.4	1812	0.37	6.7
Anch. 2	1.3	0.18	39.6	1679	10.7	0.37	31.4	1641	0.39	6.4
Anch. 3	1.4	0.2	36.4	1684	10.8	0.94	31.4	1648	0.37	6.2

Figure 4. Measured frequency response and fitted parameters of 1.864 GHz resonators in vacuum, with -10 dBm input power.

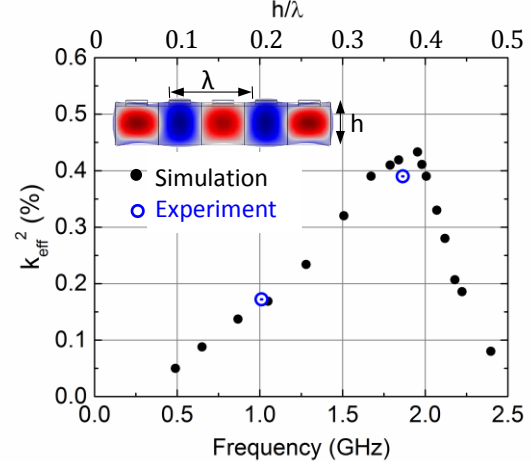


Figure 5. Simulated k_{eff}^2 dependence on the normalized GaN film thickness and frequency. Inset shows 2D Comsol simulation of S_0 mode. Experimental results are in good agreement with theory.

in Figs. 1 and 4 are overlaid in this plot, with excellent agreement between simulation and experiment. The inset of Fig. 5 illustrates the setup of the 2D simulation used to extract k_{eff}^2 . We have accounted for the thin nucleation layer at the bottom of the GaN, and for the nitride passivation layer covering the resonator. While the simulation is based on values of the piezoelectric coefficients that correspond to bulk single-crystal GaN, the thin-film material used to fabricate the resonators contains a high dislocation-density buffer region at the bottom of the stack [6]. These defects are due to the lattice mismatch between the silicon substrate and GaN and can span up to a micron of the thickness of the film. Such crystal imperfections can affect the electromechanical properties of the material, leading to modified values of the piezoelectric coefficients and as a result, lower k_{eff}^2 . However, the agreement between simulation and experiment in this work indicate that the dislocations in the GaN transition layer contribute negligibly to the transducer coupling. This highlights the potential for using the HEMT stack for bulk acoustic resonators without additional processing of the material.

V. CHARACTERIZATION

Robust filters and oscillators in wireless systems require a complete characterization of the impact of ambient conditions, such as pressure and temperature on their performance, as well as excellent power handling capabilities.

A. Pressure

The pressure dependence of the Q_m of the 1GHz 5-anchor resonator is shown in Fig. 6. While a roll-off characteristic due to Couette damping can be seen in the range 1-1000 mbar, a total drop in Q_m of only 1.5% between high vacuum and atmospheric pressure is observed. This weak dependence on ambient pressure is another benefit of high frequency bulk modes. This shows high potential for monolithic integration of GaN resonators with HEMTs, without the need for expensive, ultra-high vacuum packaging.

B. Temperature

As GaN is increasingly used in high-power applications and for operation in harsh environments, it is important to characterize the effect of temperature on the performance of these resonators. To this end, we have tested these devices over a temperature range spanning 20°C to 80°C, as shown in Fig. 7. The first order temperature coefficient of frequency (TCF) is extracted to be -24.2 ppm/°C. This is comparable with other previously reported bulk mode GaN resonators [5], as well as AlN contour modes [7]. Several groups have demonstrated temperature-compensation in AlN Lamb mode resonators that achieve a zero first order TCF, by incorporating a thin layer of silicon dioxide in the resonant

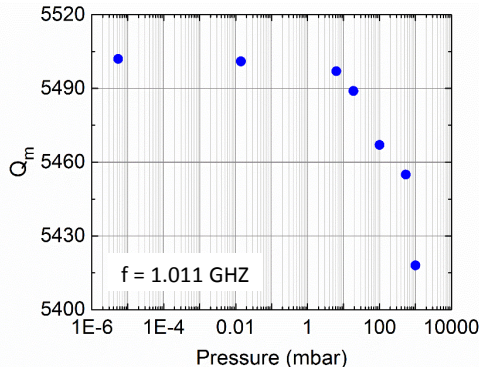


Figure 6. Measurements show a small dependence of the mechanical quality factor of the 1GHz resonator on the ambient pressure.

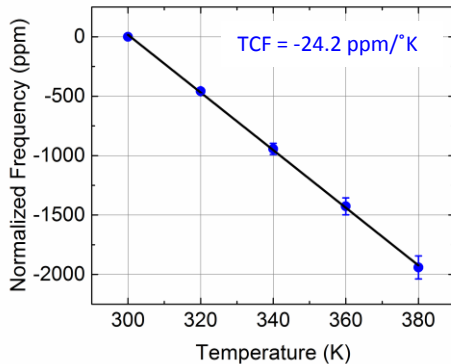


Figure 7. Experimental measurement of the temperature coefficient of frequency (TCF) for the 1GHz resonator shown in Fig. 1.

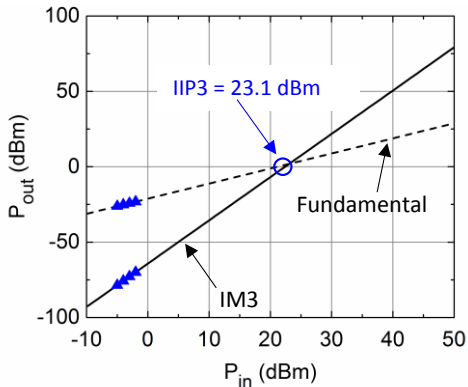


Figure 8. Power handling measurement of the resonator shown in Fig. 1, with an IIP3 of 23.1 dBm, with $19.4 \times 90 \mu\text{m}^2$ footprint.

cavity [12]. Typical HEMT processes use a thin layer of dielectric for passivation. While here we use nitride as a passivation layer, which has a negative TCF, an oxide layer can be incorporated in the passivation stack to alleviate the change in resonant frequency due to temperature shifts.

C. Power Handling

Another critical requirement for use in broadband radio communications is power handling. As bulk mode piezoelectric devices, the S_0 Lamb resonators presented here exhibit excellent power handling capabilities. Fig. 8 shows the power nonlinearity measurement of the $19.4 \times 90 \mu\text{m}^2$ 1GHz resonator in Fig. 1, with an extracted IIP3 of +23.3 dBm.

VI. CONCLUSION

We have optimized and demonstrated multiple frequency GaN Lamb mode resonators at 1-2 GHz, with the highest measured $f \cdot Q$ in GaN to date, and the highest k_{eff}^2 using IDTs without a bottom electrode, enabling tunable bandwidth filters (180-800 kHz). This was realized in a standard GaN MMIC platform, with only two additional fabrication steps. The performance of the resonators as a function of pressure and temperature has also been investigated, as well as the power handling capabilities, showing high potential for seamless integration with high power, high frequency ICs for clocking and wireless communication.

ACKNOWLEDGEMENT

We thank William Hoke, Brian Schultz and Thomas Kazior (Raytheon) for GaN growth. Fabrication took place at MIT's MTL under DARPA DAHI Foundry N66001-13-1-4022 and NSF Career ECCS-1150493 funding.

REFERENCES

- [1] M. Sawahashi, Y. Hishiyama, H. Taoka et. al., "Broadband Radio Access: LTE and LTE-Advanced", ISPACS, pp.224-227, Dec. 2009.
- [2] R. Marathe, B. Bahr, W. Wang et. al., "Resonant Body Transistors in IBM's 32 nm SOI Technology," J. MEMS, 2013, no. 99.
- [3] W.-C. Chen, C.-S. Chen, K.-A. Wen, et. al., "A generalized foundry CMOS platform for capacitively-transduced resonators monolithically integrated with amplifiers," 23rd MEMS, pp.204-207, Jan. 2010.
- [4] L.C. Popa, D. Weinstein, "Switchable piezoelectric transduction in Al-GaN/GaN MEMS resonators", 17th Transducers, pp.2461-2464, Jun. 2013.
- [5] V.J. Gokhale, J. Roberts, M. Rais-Zahed, "High performance bulk mode gallium nitride resonators and filters", 16th Transducers, pp.926-929, Jun. 2011.
- [6] O. Ambacher, "Growth and applications of Group-III Nitrides", J. Phys. D. Appl. Phys., vol. 31, pp.2653-2710, 1998.
- [7] C.-M. Lin, V. Yantchev, J. Zou et. al., "Micromachined One-Port Aluminum Nitride Lamb Wave Resonators Utilizing the Lowest-Order Symmetric Mode", J. MEMS, 2013, no 99.
- [8] A. Frangi, M. Cremonesi, A. Jaakkola et. al., "On the Optimization of Piezoelectrically Actuated MEMS Resonator", Proc. IEEE ULTSYM pp. 1043-1046, Oct. 2012.
- [9] M. Shahmohammadi, B. Harrington, R. Abdolvand, "Concurrent Enhancement of Q and Power-handling in Multi-Tether High-Order Extensional Resonators", MTT, pp.1452-1455, May 2010.
- [10] H.-S. Lee, D.S. Lee, T Palacios, "AlGaIn/GaN High Electron-Mobility Transistors Fabricated Through a Au-free Technology", Elec. Dev. Lett., vol. 32, no. 5, 2011.
- [11] IEEE Standard on Piezoelectricity, IEEESTD, 1988.
- [12] C.-M. Lin, T.-T. Yen, Y.-J. Lai et. al., "Temperature-Compensated Aluminum Nitride Lamb Wave Resonators", IEEE TUFFC, vol. 57, pp.524-532, 2010.